AMERICAN COLLEGE OF PROSTHODONTISTS®

# Cortical Bone Stress Distribution in Mandibles with Different Configurations Restored with Prefabricated Bar-Prosthesis Protocol: A Three-Dimensional Finite-Element Analysis

Erika Oliveira de Almeida, DDS, MS,[1] Eduardo Passos Rocha, DDS, MS, PhD,[2] Wirley Gonçalves Assunção, DDS, MS, PhD,[2] Amílcar Chagas Freitas Júnior, DDS, MS,[1] & Rodolfo Bruniera Anchieta, DDS[3]

[1] PhD Student in Prosthodontics, Department of Dental Materials and Prosthodontics, Aracatuba School of Dentistry, UNESP—Universidade Estadual Paulista, Brazil
[2] Associate Professor, Department of Dental Materials and Prosthodontics, Araçatuba School of Dentistry, UNESP—Universidade Estadual Paulista, Brazil
[3] PhD Student in Prosthodontics, Department of Dental Materials and Prosthodontics, Aracatuba School of Dentistry, UNESP—Universidade Estadual Paulista, Brazil

**Keywords**
Stress distribution; finite-element analysis; biomechanics; endosseous dental implantation; osseointegration; computational analysis.

**Correspondence**
Eduardo Passos Rocha, UNESP, Departamento de Materiais Odontológicos e Prótese: Rua José Bonifácio, 1193, Araçatuba- SP, cep: 16015-050, Brazil.
E-mail: eduardo_rocha@foa.unesp.br

*This study was supported by the Sao Paulo Research Foundation (FAPESP—Brazil, # 2008/00209-9).*

Accepted January 27, 2010

doi: 10.1111/j.1532-849X.2010.00656.x

## Abstract

**Purpose:** To evaluate stress distribution in different horizontal mandibular arch formats restored by protocol-type prostheses using three-dimensional finite element analysis (3D-FEA).

**Materials and Methods:** A representative model (M) of a completely edentulous mandible restored with a prefabricated bar using four interforaminal implants was created using SolidWorks 2010 software (Inovart, São Paulo, Brazil) and analyzed by Ansys Workbench 10.0 (Swanson Analysis Inc., Houston, PA) to obtain the stress fields. Three mandibular arch sizes were considered for analysis, regular (M), small (MS), and large (ML). Three unilateral posterior loads (L) (150 N) were used: perpendicular to the prefabricated bar (L1); 30° oblique in a buccolingual direction (L2); 30° oblique in a lingual-buccal direction (L3). The maximum and minimum principal stresses ($\sigma_{max}$, $\sigma_{min}$), the equivalent von Mises ($\sigma_{vM}$), and the maximum principal strain ($\sigma_{max}$) were obtained for type I (M.I) and type II (M.II) cortical bones.

**Results:** Tensile stress was more evident than compression stress in type I and II bone; however, type II bone showed lower stress values. The L2 condition showed highest values for all parameters ($\sigma_{vM}$, $\sigma_{max}$, $\sigma_{min}$, $\varepsilon_{max}$). The $\sigma_{vM}$ was highest for the large and small mandibular arches.

**Conclusion:** The large arch model had a higher influence on $\sigma_{max}$ values than did the other formats, mainly for type I bone. Vertical and buccolingual loads showed considerable influence on both $\sigma_{max}$ and $\sigma_{min}$ stresses.

Longitudinal clinical studies have confirmed higher than 90% success rates for immediate loading of implant-supported prostheses for many implant systems.[1-5] Considering that the main purpose of the prefabricated bar is its use under immediate loads, primary implant stability is an important factor for successful osseointegration.[6] The prefabricated bar has predictable levels of adaptation and passivity, diminishing treatment time;[7] however, the mandible must show sufficient volume and bone density to receive the implants.[8] Its anatomical thickness is crucial and must be compatible with the form of the bar.

The influence of horizontal mandibular arch shape on bone stress distribution has not been clearly discussed by previous literature. The prefabricated bar can adapt itself to the mandibular arch format on the horizontal plane; however, the bar shape may not adjust, with mandibular arches exhibiting dimensional variations, resulting in implants poorly covered by cortical bone and influencing the treatment success rates.

Therefore, the purpose of this study was to evaluate bone stress distribution using three-dimensional finite element analysis (3D-FEA) in three horizontal sizes of a mandibular arch (small, regular, large) restored by a prefabricated bar-prosthesis protocol with four implants.

## Materials and methods

A representative model (M) of a mandibular arch was created according to the anatomical data of a completely edentulous mandible[9] exhibiting transversal section type III[10] using SolidWorks 2010 software (Inovart, São Paulo, Brazil). The cortical bones simulated were type I (M.l) and type II (M.ll)[11] based on the elastic modulus of the mandibular bone, according to Tada et al[15] (Table 1). The horizontal dimension of the mandible was increased and reduced by 11% to obtain large (M.lL and M.llL) and small (M.lS and M.llS) horizontal dimension models (Fig 1). These percentage differences were established according to the maximum possible limits for mandible size modification, while still guaranteeing total covering of the implant screws in the buccal and lingual faces.

Each mandibular arch was restored with a prefabricated-bar system using four interforaminal implants (Neopronto prefabricated-bar system, Neodent, Implante Osseointegráveis, Curitiba, Brazil) placed at the same location for each model (Fig 2). The implants (4.00-diameter × 13.00-mm length) were cylindrical, with a single body, and were placed in parallel according to the orientation of the prefabricated bar. The prefabricated-bar system shows specific components for retaining the bar on the implants (Figs 2A,B), with cylinders to be screwed under implants. The bar was cemented under those cylinders. The resin cement layer of 0.05 mm[12] was virtually simulated by using Panavia F (Kuraray Co, LTD, Osaka, Japan). Additional screw retainers can be used to stabilize the bar. The bar was placed under those four implants (Fig 2C).

Due to variation in dimensions, the two most posterior implants were positioned closer to the buccal and lingual sides for the small (M.lS and M.llS) and large (M.lL and M.llL) mandible sizes, respectively. The implants were numbered one to four from right to left (Fig 2B).

The mechanical properties (Elastic modulus [E] and Poisson ratio [$\nu$]) were incorporated according to previous literature (Table 1). The materials were homogeneous, isotropic, and linearly elastic; however, the elastic modulus of the cortical bone varied to better represent the different types of bone (I and II) in the mandible.[15] The bone-implant interface was considered perfectly integrated.

A solid parabolic tetrahedral element[13] with 0.1 mm-sized elements was used for meshing. The mesh refinement was established based on the convergence of analysis (6%).[14] The models had between 302,412 and 316,229 nodes and between 182,032 and 195,846 elements. All nodes at the posterior surface of each model were fixed along the $x$, $y$, and $z$ coordinates to simulate the continuity of the mandibular ramus, as well as the nodes at the base to avoid inertial movement and simulate muscle support (Fig 3).[16] Three unilateral posterior loads (L) (150 N)[16,17] were used: perpendicular to the prefabricated bar (L1),[18] 30° oblique in a buccolingual direction (L2),[18] and 30° oblique in a lingual-buccal direction (L3) (Fig 2D).

ANSYS Workbench 10.0 software (Swanson Analysis Inc., Huston, PA) was used to obtain the stress fields (Fig 4). Although von Mises stress criteria have been obtained in some studies,[19-24] maximum and minimum principal stresses ($\sigma_{max}$, $\sigma_{min}$), equivalent von Mises stress ($\sigma_{vM}$), and maximum principal strain ($\varepsilon_{max}$) were obtained for all conditions. Maximum principal stress was selected because the bone shows large differences between the ultimate tensile and compressive strengths.[25,26] The influence of all loads was evaluated at the bone-implant interface around implant number four.

**Table 1** Material properties

| Material | Young's modulus (GPa) | Poisson's ratio |
|---|---|---|
| Type I bone[15] | 9.5 | 0.3 |
| Type II bone[15] | 5.5 | 0.3 |
| Cortical bone[32] | 13.7 | 0.3 |
| Titanium[14] | 110 | 0.35 |
| Cementing layer[12] | 18.3 | 0.3 |

## Results

The maximum and minimum principal stresses ($\sigma_{max}$, $\sigma_{min}$) were highest in the large mandibular arch, followed by the small and regular mandibular arches. For type I bone models, M.IL showed the highest $\sigma_{max}$ values (MPa) (12.3 for L1, 35.1 for L2), followed by M.I (6.98 for L1, 31.8 for L2), and M.IS (3.93 for L1, 28 for L2) (Fig 5). In the regular and small mandibular arches, $\sigma_{max}$ decreased by 43.25% and 68.04%, respectively, for L1 and by 9.40% and 20.22%, respectively, for L2, compared with the large mandibular arch. On the other hand, M.IS showed the highest $\sigma_{max}$ for L3 (−16.6 MPa), followed by M.IL (−13.9 MPa), and M.I (−0.31 MPa) (Fig 5).

For type II bone models, M.IIL and M.IIS showed the highest $\sigma_{max}$ for L1 and L3 (M.IIL -7.08 MPa, M.IIS -7.03 MPa for L1; M.IIL -17.20 MPa for L3) (Fig 6). The highest $\sigma_{max}$ for L2 was noted in M.II (27.9 MPa) (Fig 6). In L2, $\sigma_{max}$ decreased for M.IIS and M.IIL (26.16%) compared with M.II.

Tensile stress was more evident than compression stress in type I bone (Fig 5). Similar behavior was observed in type II bone; however, the stress values were lower than those in type I bone (Fig 6).

For the maximum principal strain ($\varepsilon_{max}$), M.IS showed the highest stress (−2.2 for L1, 0.68 for L3), followed by M.IL (1.05 for L1, 0.53 for L3), and M.I (0.99 for L1, 0.55 for L3). For L3, M.IL showed a lower $\varepsilon_{max}$ than M.I. For L2, M.IL showed an $\varepsilon_{max}$ peak of 2.73 followed by M.I (2.37) and M.IS (2.07). When the small mandibular arch was used, $\varepsilon_{max}$ increased by 55% for L1 in comparison with M.I and 22.05% for L3 in comparison with the large mandibular arch. For the L2 condition, the small mandibular arch showed the lowest values in comparison with the large (23.44%) and regular mandibular arches (11.81%).

For type II bone models, M.II and M.IIL showed the highest and similar $\varepsilon_{max}$ (0.92) for L1. The same was observed for M.IIS and M.IIL (0.53) for L3, followed by M.IIS (0.79 for L1) and M.II (0.45 for L3). The $\varepsilon_{max}$ decreased in M.IIS (14.13% for L1) and M.II (15.09% for L3). For L2, M.II showed the highest $\varepsilon_{max}$ (2.12), followed by M.IIS and M.IIL (2.07).

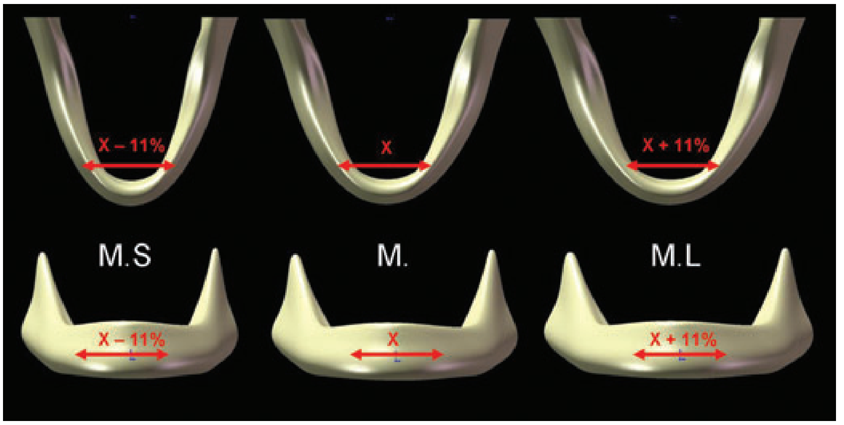


**Figure 1** Configuration of the mandibular arch on the horizontal plane. Abbreviations: M.S, small interforaminal dimension; M., regular interforaminal dimension; M.L, large interforaminal dimension.

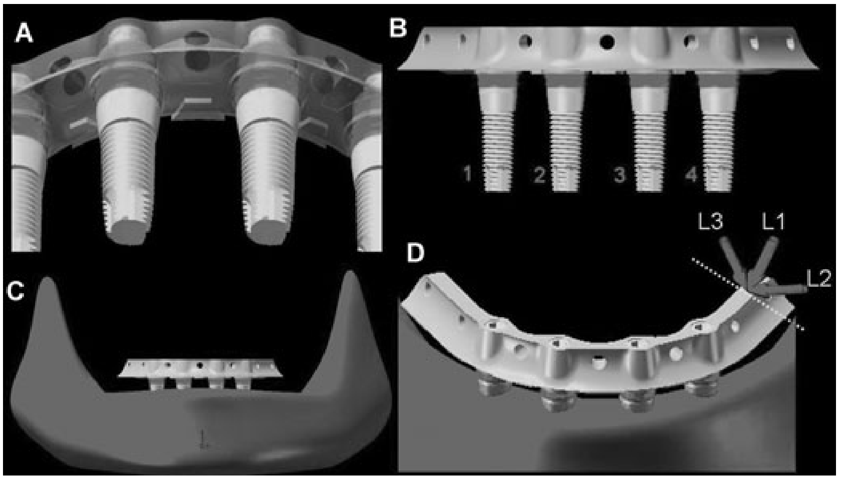


**Figure 2** (A and B), frontal and inferior views, respectively, of the implants connected to the prefabricated bar; (B), 1-4: Implant identification; (C), finalized model; (D), L1 (axial load), L2 (buccolingual load), and L3 (lingual-buccal load).

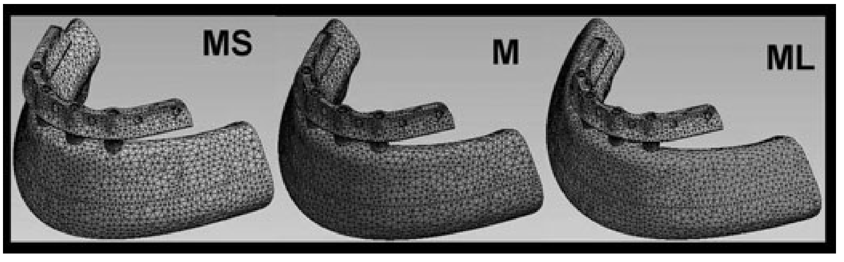


**Figure 3** Finite-element meshes of the small (M.S), regular (M.), and large (M.L) formats.

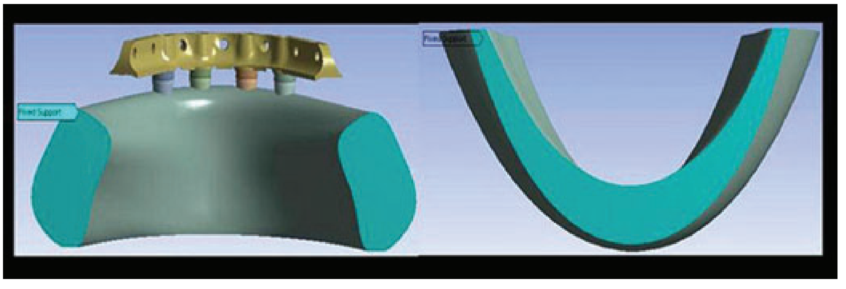

**Figure 4** Boundary conditions in the finite elements program.

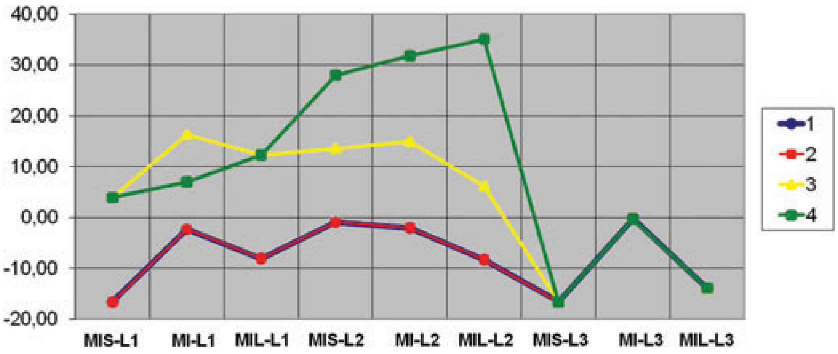


**Figure 5** Values of $\sigma_{max}$ (MPa) for cortical bone in M.IS, M.I, and M.IL after L1, L2, and L3. The numbers 1, 2, 3, and 4 represent implants from right to left, respectively. Abbreviations: M.IS, type I small format; M.I, type I regular format; M.IL, type I large model format; L1, axial load; L2, lingual-buccal load; L3, buccal-lingual load.

The influence of mandible size on $\sigma_{max}$ and $\sigma_{strain}$ was most evident in the L1 and L3 conditions. For both $\sigma_{max}$ and $\sigma_{strain}$ the alterations in mandible size showed little influence on the stress values for L2.

The equivalent von Mises ($\sigma_{vM}$) shows similar results between the large and small mandibular arches for L1, L2, and L3. Regular arches showed the lowest values in type I bone and similar values for the small and large mandibular arches in type II bone. The L2 condition showed highest values for all parameters ($\sigma_{vM}$, $\sigma_{max}$, $\sigma_{min}$, $\varepsilon_{max}$).

## Discussion

Although no studies have evaluated the effects of different mandibular arch sizes in completely edentulous patients undergoing osseointegrated implant treatment, there is still a clinical concern about the use of prefabricated bars, even under adequate bone volume and shape conditions.[27] This study showed the influence of differences in mandibular size (small, regular, and large) on the alteration of stress in implants placed in the posterior region (implant number four). This area is subject to the highest linear dimension modifications due to different horizontal mandibular arch formats.

A mandible with implants closer to the buccal or lingual bone limits might show higher stress concentration in comparison to the regular size. In the long term, this might lead to bone loss.[28]

The vertical loading generated equivalent von Mises stress concentration at the lingual face of the bone for all models. It was highest for the small mandibular arch type I. When the buccolingual load was applied, the stress was concentrated at the buccal, lingual, and distal sides of implant number four. The large mandibular arch type I showed the highest stress concentration in that area. When the lingual-buccal load was applied, the stress concentration occurred at the mesial and distal sides of the implant. The small mandibular arch type I showed the highest stress concentration.

Although mandible size might explain the difference in location and stress intensity based on loading variation, the stress for the L2 condition showed small differences between models, with similar values in comparison to L1 and L3 conditions. Studies on the shape of triangular and square arch formats are necessary to better understand the influence of mandible configuration with regards to implant position. The phenomenon of bone remodeling may be particularly associated with external geometric changes in the bone;[29] however, no data have been shown in previous literature that confirm exactly how mechanical loads are transmitted to the osteoblasts and osteoclasts for the process of bone remodeling to occur.[29,30]

The use of oblique loads in FEA simulates a more realistic stress-distribution situation, which is capable of demonstrating localized cortical bone stress.[31] Numerical analysis shows advantages over other methods for characterizing complex clinical situations, showing a high degree of sensitivity to parameters such as load, shape conditions, and material properties, with adequate reliability among models.[18,32] It is also worth highlighting the benefit of the modeling technique used in this study. Even though solid models can be created from CT,[33] altering the horizontal dimension of the bone is not a simple procedure in such models. In the technique used in this study, the shapes of the transversal sections of the mandibular bone

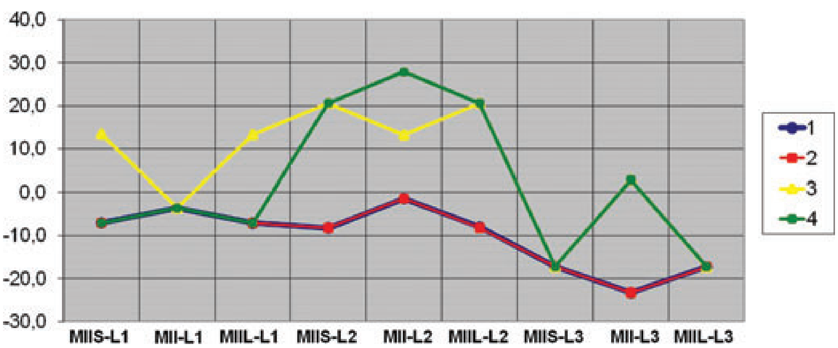


**Figure 6** Values of $\sigma_{max}$ (MPa) for cortical bone in M.IIS, M.II, and M.IIL after L1, L2, and L3. The numbers 1, 2, 3, and 4 represent implants from right to left, respectively. Abbreviations: M.IIS, type II small format; M.II, type II regular format; M.IIL, type II large format; L1, axial load; L2, lingual-buccal load; L3, buccal-lingual load.

were very similar across models, making the interforaminal distance the influencing factor of stress alteration; however, it must be emphasized that the structures were assumed to be homogeneous, isotropic, and linearly elastic, but, in fact, the properties of the materials are different. Cortical bone is a transversally isotopic and nonhomogeneous structure.[34] This should be considered in future studies. Furthermore, the assumption that all the interfaces (including bone-implant interface) were perfectly bonded cannot always be transferred to real clinical situations, as osseointegration does not occur between surfaces with perfect contact interface,[30] an issue that requires further investigation. Although the reliability might be affected, experimental data (ie, the use of strain gauges) are also necessary to evaluate bone behavior based on different arch configurations to add further data to such investigations.

## Conclusions

According to the methodology used, it was concluded that:

(1) The large arch format showed higher influence on the stress variation compared with other formats; mainly for type I bone.
(2) For type II bone, the large and small arch sizes showed similar stress values, which were larger than those in the regular-sized format.
(3) Vertical and buccolingual loads showed the most influence on the alteration of $\sigma_{\text{max.}}$
(4) The small type I bone format showed greater deformation compared to the other formats when vertical and lingual-vestibular loads were applied.

## Acknowledgments

We thank Neodent Implante Osseointegráveis (Curitiba, PR, Brazil) for supplying the implant system used in this research study.

## References

1. Jaffin RA, Kumar A, Berman CL: Immediate loading of dental implants in the completely edentulous maxilla: a clinical report. Int J Oral Maxillofac Implants 2004;19:721-730
2. Castellon P, Block MS, Smith MB, et al: Immediate loading of the edentulous mandible: delivery of the final restoration or a provisional restoration – which method to use? J Oral Maxillofac Surg 2004;62:30-40
3. Engquist B, Astrand P, Anzén B, et al: Simplified methods of implant treatment in the edentulous lower jaw: a 3-year follow-up report of a controlled prospective study of one-stage versus two-stage surgery and early loading. Clin Implant Dent Relat Res 2005;7:95-104
4. Ercoli C, Romano PR, Al Mardini M, et al: Restoration of immediately placed implants in 3 appointments: from surgical placement to definitive prostheses. J Prosthet Dent 2006;96:212-218
5. Misch CE: Density of bone: effect on treatment plans, surgical approach, healing, and progressive bone loading. Int J Oral Implantol 1990;6:23-31
6. Simamoto PC, Davi LR, Gomes VR, et al: Immediate function in the edentulous mandible: replacement of a lost implant using prefabricated guides. J Prosthet Dent 2006;95:161-164
7. Hatano N, Yamaguchi M, Suwa T, et al: A modified method of immediate loading using Brånemark implants in edentulous mandibles. Odontology 2003;91:37-42
8. Parel SM, Ruff SL, Triplett RG, et al: Bone reduction surgical guide for the Novum implant procedure: technical note. Int J Oral Maxillofac Implants 2002;17:715-719
9. Sicher H, Dubrul EU: Oral Anatomy. St. Louis, Mosby, 1989, pp. 28–30
10. Quirynen M, Mraiwa N, van Steenberghe D, et al: Morphology and dimensions of the mandibular jaw bone in the interforaminal region in patients requiring implants in the distal areas. Clin Oral Implants Res 2003;14:280-285
11. Truhlar RS, Orenstein IH, Morris HF, et al: Distribution of bone quality in patients receiving endosseous dental implants. J Oral Maxillofac Surg 1997;55:38-45
12. Li LL, Wang ZY, Bai ZC, et al: Three-dimensional finite element analysis of weakened roots restored with different cements in combination with titanium alloy posts. Chin Med J 2006;119:305-311
13. Cook RD, Malkus DS, Plesha ME: Concepts and Applications of Finite Element Analysis. New York, Wiley, 2001, pp. 542-573
14. Huang HL, Hsu JT, Fuh LJ, et al: Bone stress and interfacial sliding analysis of implant designs on an immediately loaded maxillary implant: a non-linear finite element study. J Dent 2008;36:409-417
15. Tada S, Stegaroiu R, Kitamura E, et al: Influence of implant design and bone quality on stress/strain distribution in bone around implants: a 3-dimensional finite element analysis. Int J Oral Maxillofac Implants 2003;18:357-368
16. Ding X, Zhu X-H, Liao SH, et al: Implant-bone interface stress distribution in immediately loaded implants of different diameters: a three-dimensional finite element analysis. J Prosthodont 2009;18:393-402
17. Lin CL, Wang JC, Ramp LC, et al: Biomechanical response of implant systems placed in the maxillary posterior region under various conditions of angulation, bone density, and loading. Int J Oral Maxillofac Implants 2008;23:57-64
18. Yokoyama S, Wakabayashi N, Shiota M, et al: Stress analysis in edentulous mandibular bone supporting implant-retained 1-piece or multiple superstructures. Int J Oral Maxillofac Implants 2005;20:578-583
19. Akimoto M, Oka T, Oki K, et al: Finite element analysis of effect of softness of cushion pads on stress concentration due to an oblique load on pressure sores. J Nippon Med Sch 2007;74:230-235
20. Bonivtch AR, Bonewald LF, Nicolella DP: Tissue strain amplification at the osteocyte lacuna: a microstructural finite element analysis. J Biomech 2007;40:2199-2206
21. Ichim I, Swain M, Kieser JA: Mandibular biomechanics and development of the human chin. J Dent Res 2006;85:638-642
22. Akiko K, Nagasao T, Kaneko T, et al: A comparative study of most suitable miniplate fixation for mandibular symphysis fracture using a finite element model. Keio J Med 2006;55:1-8
23. Nomoto S, Matsunaga S, Ide Y, et al: Stress distribution in maxillary alveolar ridge according to finite element analysis using micro-CT. Bull Tokyo Dent Coll 2006;47:149-156
24. Zhiyong L, Arataki T, Shimamura I, et al: The influence of prosthesis designs and loading conditions on the stress

distribution of tooth-implant supported prostheses. Bull Tokyo Dent Coll 2004;45:213-221
25. Furmanski J, Anderson M, Bal S, et al: Clinical fracture of cross-linked UHMWPE acetabular liners. Biomaterials 2009;30:5572-5582
26. Ciftçi Y, Canay S: The effect of veneering materials on stress distribution in implant-supported fixed prosthetic restorations. Int J Oral Maxillofac Implants 2000;15:571-582
27. Klee de Vanconcellos D, Bottino MA, Saad PA, et al: A new device in immediately loaded implant treatment in the edentulous mandible. Int J Oral Maxillofac Implants 2006;21:615-622
28. Li J, Li H, Shi L, et al: A mathematical model for simulating the bone remodeling process under mechanical stimulus. Dent Mater 2007;23:1073-1078
29. Huiskes R, Weinans H, Grootenboer HJ, et al: Adaptive bone-remodeling theory applied to prosthetic-design analysis. J Biomech 1987;20:1135-1150
30. Holmes DC, Loftus JT: Influence of bone quality on stress distribution for endosseous implants. J Oral Implantol 1997;23:104-111
31. Bozkaya D, Muftu S, Muftu A: Evaluation of load transfer characteristics of five different implants in compact bone at different levels by finite elements analysis. J Prosthet Dent 2004;92:523-530
32. Sevimay M, Turhan F, Kiliçarslan MA, et al: Three-dimensional finite element analysis of the effect of different bone quality on stress distribution in an implant-supported crown. J Prosthet Dent 2005;93:227-234
33. Cattaneo PM, Melsen B: The use of cone-beam computed tomography in an orthodontic department in between research and daily clinic. World J Orthod 2008;9:269-282
34. Cochran DL: The scientific basis for and clinical experiences with Straumann implants including the ITI dental implants system: a consensus report. Clin Oral Implants Res 2000;11:33-58